



# IJRASET

International Journal For Research in  
Applied Science and Engineering Technology



---

# INTERNATIONAL JOURNAL FOR RESEARCH

IN APPLIED SCIENCE & ENGINEERING TECHNOLOGY

---

**Volume: 8      Issue: II      Month of publication: February 2020**

**DOI: <http://doi.org/10.22214/ijraset.2020.2023>**

**[www.ijraset.com](http://www.ijraset.com)**

**Call:  08813907089**

**E-mail ID: [ijraset@gmail.com](mailto:ijraset@gmail.com)**

# Design and Analysis of a Nano satellite for Space Debris Detection and Removal

Lekshmi K Ravi<sup>1</sup>, Anishma Uday<sup>2</sup>, Susan Ligori M<sup>3</sup>, Karthikeyan L M<sup>4</sup>

<sup>1, 2, 3, 4</sup>Department of Aerospace Engineering, Noorul Islam Centre For Higher Education

**Abstract:** *The aim of the paper is to design and analyze a nanosatellite for space debris detection and removal. Space debris is becoming a huge problem in the field of space explorations. The debris that surrounds the planet earth is also creating huge pollution problems. It is becoming a serious crisis and increasing the chance of accidents when planning to launch new missions. By adding the features to detect the presence of this hazardous space waste in a satellite and the method to remove it, we can achieve clear and accident free space navigation. To achieve this aim, ASTRAA NANOSAT is designed and analyzed using CATIA V5 and Nastran Patran software.*

**Keywords:** *Space debris, Design, Nanosatellite, CATIA V5, Nastran Patran, Analysis, Components used*

## I. INTRODUCTION

Space debris otherwise called space junks, trash or garbage is becoming a serious threat to the space exploration in the present era. Space debris is unusable satellites, parts or fragments produced due to collisions, tools dropped intentionally or accidentally, or even the dust of minute particles (Habimana Sylvestre, 2017)[1]. Most of them are occupied at lower Earth orbits and are becoming a threat to the upcoming space missions and existing satellites in space. As of January 2019, more than 128 million bits of debris which are less than 1cm were estimated (D Mahrholz, 2002)[2]. Space debris is extended over 160km to 36000km above the Earth's surface (Christoph R Englert, 2014)[3].

The tracking and cataloguing of space debris are efficiently done by the US Space surveillance Network. But they give priority to only objects ranging between 5cm to 10cm sized with the help of large number of optical sensors and radars. The space debris can be classified based on their size and impacts.

Those which are having very small size will cause more impact since they can even move at a speed of around 20 times the speed of bullet. In order to prevent the collisions with these objects, satellites and space stations have their own orbital manoeuvring and protection systems (Ansdell.M, 2010)[4].

International Space Station was in the fear of a debris collision in 2011. Space station is also under the threat of this dangerous issue since it orbits in 300- 400 Kilometre range.

New technologies are being developed and studied regarding the complete removal and prevention of space debris (K Wormnes, 2013)[5]. According to IADC (Inter-Agency Space Debris Coordination Committee), fifty third session of scientific and technical subcommittee United Nations Committee on the peaceful uses of outer space 2016, the highly effective management method we can adopt is the limitation of probability of accidental collisions.

Even the orbital manoeuvring technique also has some draw backs. One of the important problems that we face nowadays is that we don't have practicing or existing technologies which are able to detect the debris with size less than one centimetre. There is no international treaty yet to limit space debris, voluntarily guidelines have been published by the United Nations Committee on the peaceful uses of outer space.

## II. METHODOLOGY

The ASTRAA NANOSAT has been designed in CATIA V5 software. The complicated structures can be easily designed and modified in this software. With the help of different work benches including the sketcher, part design and assembly the components are designed individually and assembled it. Lots of information regarding each electronic components which need to be used, the materials suitable for the structures, the specifications of each components, the launch vehicle to be used and the load satellite can occupy are collected. The overall weight and Centre of gravity of the satellite has been calculated and analysed using NASTRAN PATRAN software.

### III.COMPONENTS USED

As per requirements, lots of electronic components are used in the satellite which includes the following,

#### A. Sun Sensor

Sun sensors are inevitable parts of Attitude and Orbital Control System (AOCS). In order to achieve the effective orientation of the satellite, for proper working of solar panels and for the overall stability of the satellite four sun sensors are implemented two in left side panels and the two in right side panels. Specifications are given in table 1. (Shaobo Ni, 2011) [6] Fig 3.1 shows the model of sun sensor designed in CATIA V5 software.

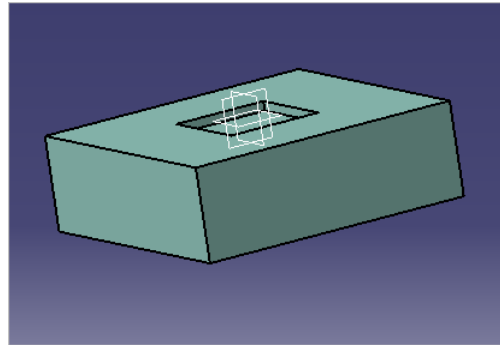


Fig.1 model of sun sensor designed in CATIA V5software

#### B. Star Trackers

Star trackers are parts of AOCS. They are able to identify thousands of stars and are used as absolute attitude sensors. As per the requirements, a pair of star trackers is used in the satellite, which is placed in the top deck of the satellite (Delabie, 2016)[7]. Specifications are given in table 1. Fig 3.2 shows the Model of star tracker designed in CATIA V5 software.

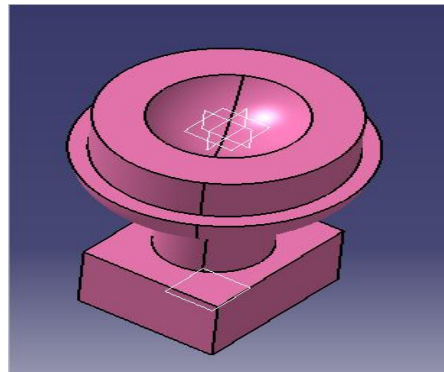


Fig.2 model of star tracker designed in catia v5 software

#### C. Magnetometers

It is an attitude sensor which is an integral part of AOCS. They can effectively measure earth's geomagnetic field. For the particular application 2 magnetometers are implemented in the top panel of the satellite with the help of an ejection stand (Halil Ersin Soken, 2015)[8].Specifications are given in table 1.

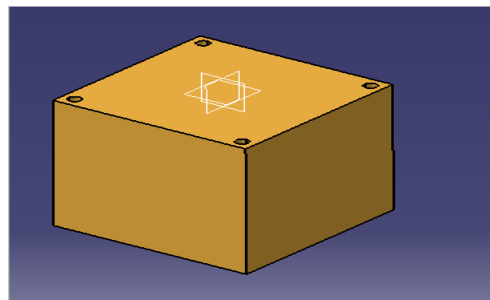


Fig.3 model of magnetometer designed in catia v5 software

#### D. Magnetic Torquer

Magnetic torquer is an AOCS system, which is built from electromagnetic coils. It creates magnetic dipole moment between satellites and earth by producing a magnetic field around the satellite. Because of this moment a torque is created in the satellite. Specifications are given in table 1.( Kikuko Miyata, 2009)[9] Fig 3.4 shows the model of magnetic torquer designed in CATIA V5 software.

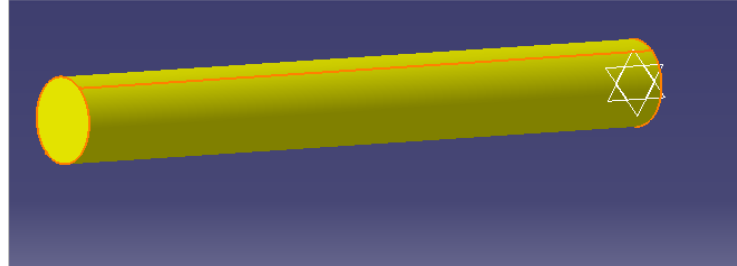


Fig.4 model of magnetic torquer designed in catia v5 software

#### E. Gyroscope

It is an absolute attitude sensor which plays a relative role in the de-tumbling process of the satellite. It is able to reduce the angular velocity of the satellite whenever it is in rotation. (Shaobo Ni, 2011)[10]. Specifications are given in table 1.

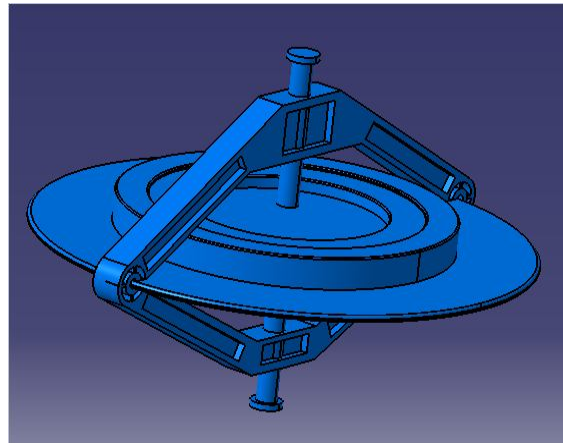


Fig.5 model of the gyroscope designed in catia v5 software

#### F. Reaction Wheel

It is an actuator of AOCS. This will help in turning the satellites in small orientations for example to point the sensors to the exact location of an object. They are equipped with an electric motor. It can only rotate the spacecraft around its center of mass and not capable of moving the spacecraft from one place to another. It is also used for the de tumbling of the satellite and to achieve three axes stabilized condition. Specifications are given in table 1. (Long, 2014)[11].

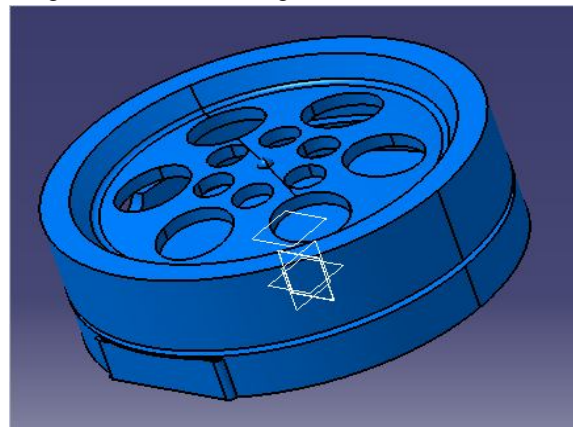


Fig.6 model of the reaction wheel designed in catia v5 software

### G. Solar Panels

For getting the maximum output solar panels should be perpendicular to the sun rays. The cells of the panels can have a size ranging from 1\*1cm, 2\*6cm or 3\*3cm. The cell thickness should not be less than 0.10mm thickness. Electricity produced by a panel is proportional to the surface area. Hence for getting more power we can either increase the surface area or can increase the cell numbers. (Touhidul Alam, 2018)[12]. Specifications are given in table 1.

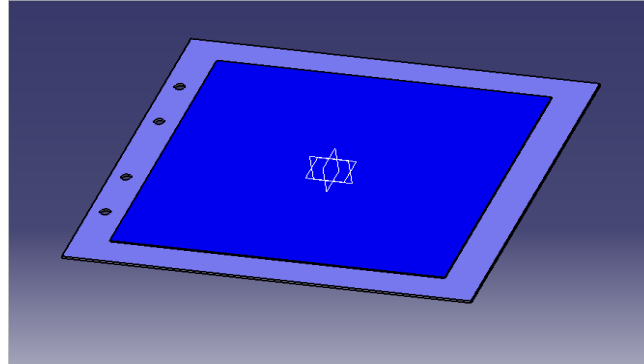


Fig.7 model of the solar panel designed in catia v5 software

### H. Global Positioning System

It is not required that GPS should always point the ground. Since, we are having antennas for effective transmission and reception. GPS should be placed apart from the shadow of other system. The initial signal for the GPS is provided from the ground through OBC. Specifications are given in table 1. (Erin Kahr, 2013)[13].

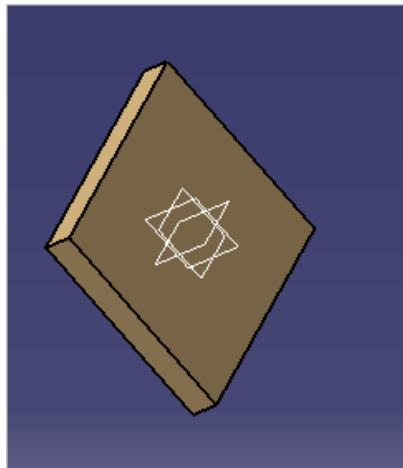


Fig.8 model of the gps system designed in catia v5 software

### I. Battery

Two Lithium ion batteries are used in ASTRAA NANOSAT. Specifications are given in table 1. (Fabio Santon, 2002)[14].

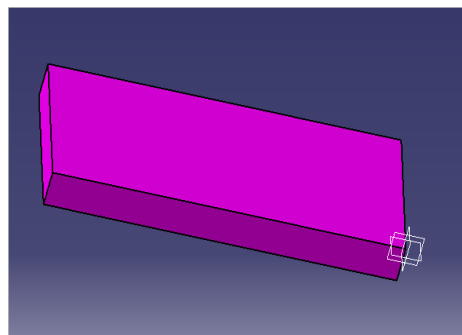


Fig.9 model of the battery designed in catia v5 software

### J. Onboard Computer

The on board computer (OBC) provide complete solution for the signal processing and communication interfaces for the various subsystems of ASTRAA NANOSAT. The OBC monitor the processor health status of each subsystem and triggers the isolation of the faulty subsystem. (Saurabh M Raje, 2017)[15] Specifications are given in table 1.

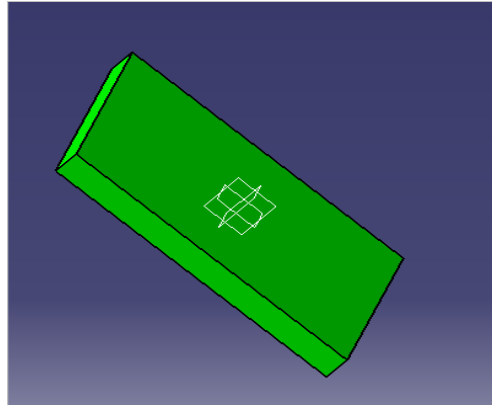


Fig.10 model of the onboard computer designed in catia v5 software

### K. S Band Antenna

It is an integral part of Telecommand and Telecommunication system (TTC) which enables effective communication of the satellite with ground station. (M.T. Islam, 2015)[16]. Specifications are given in table 1.

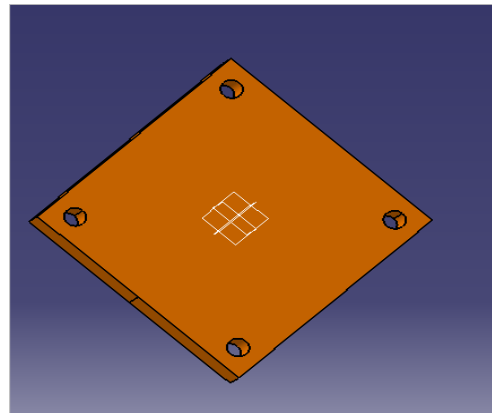


Fig.11 model of the s band antenna designed in catia v5 software

### L. UHF and VHF Antenna

VHF and UHF antenna comes under Telemetry and Telecommand subsystem. These two antennas provide proper communication signals for the satellite and ground station. (Wilke, 2015)[17] Specifications are given in table 1.

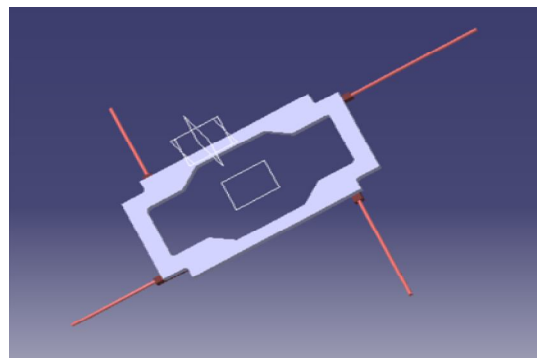


Fig.12 model of the vhf and uhf antenna designed in catia v5 software

#### M. Power Distribution Module (PDME)

Power distribution module usually comes under the Electric Power System of a satellite. This module generally consists of three important parts. They are power supply, current-limit switches and power monitoring. (A. Elmayh, 2017)[18] Specifications are given in table 1.

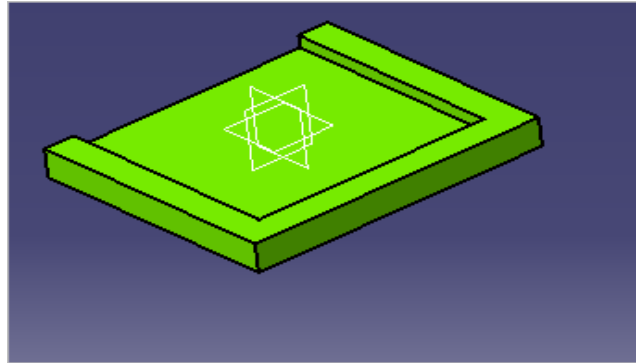


Fig.13 model of the PDME designed in catia v5 software

#### N. Telemetry and Telecommand System (TTC)

The telemetry and telecommand system is the system which provides the telecommunication link between the satellite and the ground station. The TTC collects the data from the sensors which contains the data about the satellite and send it to the ground station. This subsystem consists of telemetry, tracking and command subsystems. Specifications are given in table 1.

(Jie Liu, 2012)[19] (preliminary design review document for NIUSAT telemetry telecommand and communication system(TTC), 2013)

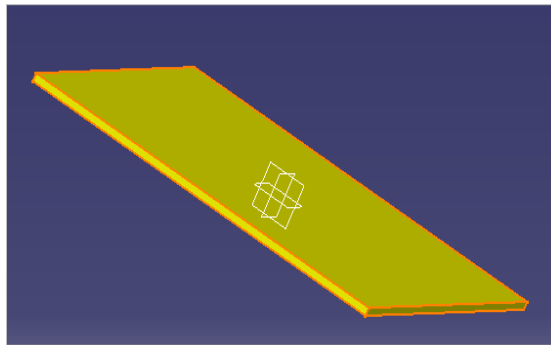


Fig.14 model of ttc module designed in catia v5 software

#### O. Pulse Plasma Thruster (PPT)

It is a simplest form of electric spacecraft propulsion. It uses Teflon as solid propellant. Arc of electricity is passed through the material causing ablation and sublimation process. As a result gas is turned into plasma with a very high thrust. (Eslava, 2014)[20] Specifications are given in table 1.

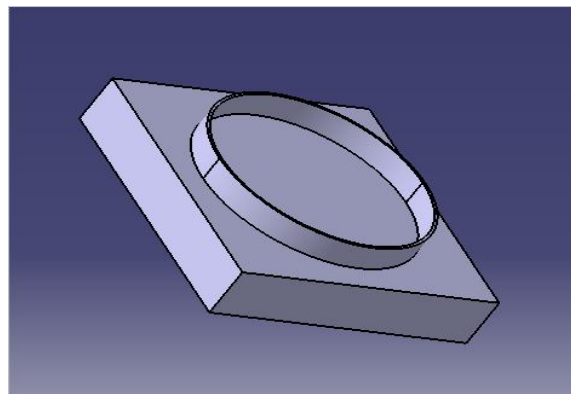


Fig.15 model of ppt designed in catia v5 software

*P. Case and Lid of Tether net*

A case is provided for keeping the tether net attached to a lid, in the satellite which is a hollow cylinder in configuration. (Benchamin Thomas, 2016)[21].

Overall weight of tether net is 3kg.

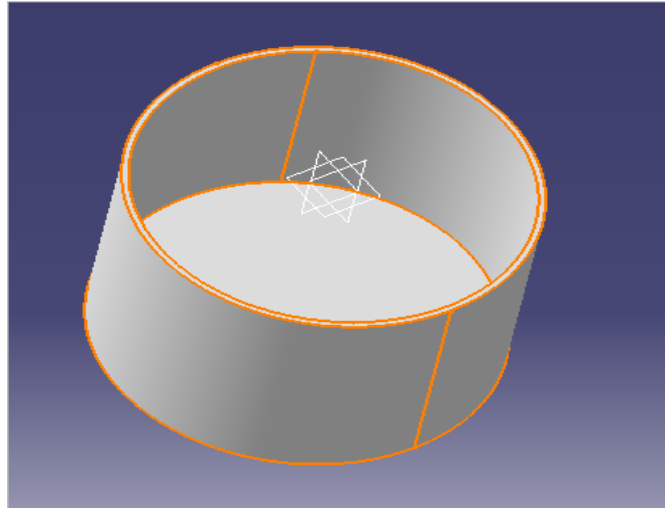


Fig.16 model of the tether net case designed in catia v5 software

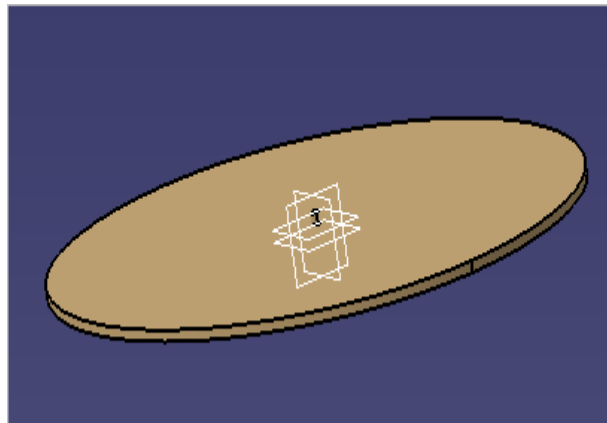


Fig.17 model of tether net lids designed in catia v5 software

*Q. Infrared Sensor (IR)*

The IR sensors will do the detection of the debris particle.

Overall weight of IR sensor is 2kg. Specifications are given in table1.

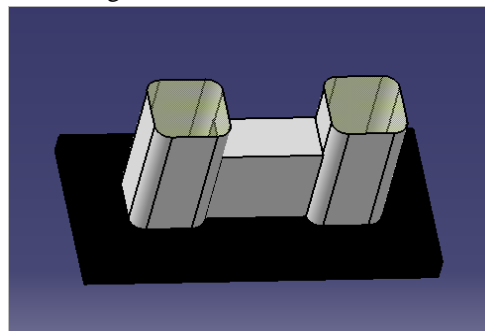


Fig.18 model of ir sensor designed in catia v5 software



Table 1  
Component Description

S.No	Name of component	Weight (gram)	Power (Watt)	Dimensions (millimeter)	Number
1	Sun sensor	6	0.175	30*30*10	4
2	Star tracker	193	1.25	50*60*93	2
3	Magnetometer	16	2	23*23*23	2
4	Gyroscope	16	0.35	23*23*23	1
5	Reaction wheel	200	0.7	50*50*30	4
6	Solar panels	800	40	480*240	4
7	Magnetic torquer	40	1.4	11*90	1
8	GPS	2.1	0.158	24*20*2.7	1
9	Battery	250	40	36*20*10	2
10	S band antenna	64	4	100*100*15	1
11	PPT	280	2	31.75*31.75*15.875	1
12	UHF VHF transceiver	94		95*46*15	1
13	S band transmitter	120	13	95*46*15	1
14	Onboard computer	900	1.5	60*60*5	2
15	Infrared sensor	2000			1
16	Tether net	3000			1
17	PDME	900	50.4	90.17*90.81*9.21	1
18	TTC	500	44	90.81*85.14*1.60	2

The overall structure of satellite is cuboid in configuration which is divided into three internal decks for the effective arrangement of components. They are top, bottom and middle deck. Cut outs are provided in the structure itself for PPT, Star trackers and IR sensors. The above components are designed in the part design work bench of the software. The top, bottom and side walls are designed and the structure was assembled in the assembly work bench of the software.

For all subsystems in ASTRAA NANOSAT, a main and reductant systems are provided.

The overall size of the satellite is 270\*270\*190(mm). Fig3.Flow diagram of the overall arrangements of various components in ASTRAA NANOSAT

#### IV. THE OVERALL STRUCTURAL DESIGN

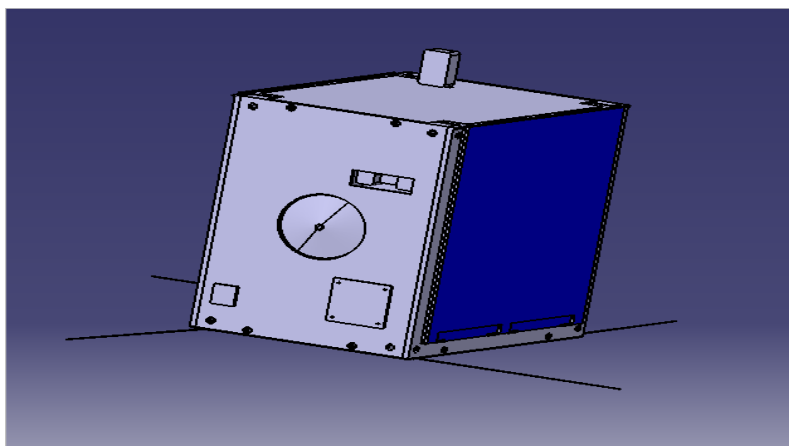


Fig.19 the overall structure of nanosatellite designed in catia v5 software

The overall structural arrangement is the assembly of the top, sides and bottom walls. The components including sun sensors, s band antenna, UHF, VHF antenna and the GPS systems are placed in the side walls, front and back walls. Four solar panels as a pair two are placed in the opposite side walls which are flexible. Magnetometers are placed at the top panel with the help of an ejection stands. Tether net case and the lid attached to it are provided in the front wall of the satellite. The magnetic torquer coils are placed at the bottom of the four walls.

PPT is placed at the back wall of the satellite and the IR sensors are placed at the front panel. The star trackers and gyroscope are placed at the top and middle decks respectively. (Jonathan Becedas, 2018) [22] Fig 19. Shows the overall structural design of nanosatellite designed in CATIAV5 software and Fig 21. Shows the rendered model of the nanosatellite done in Key shot 7.

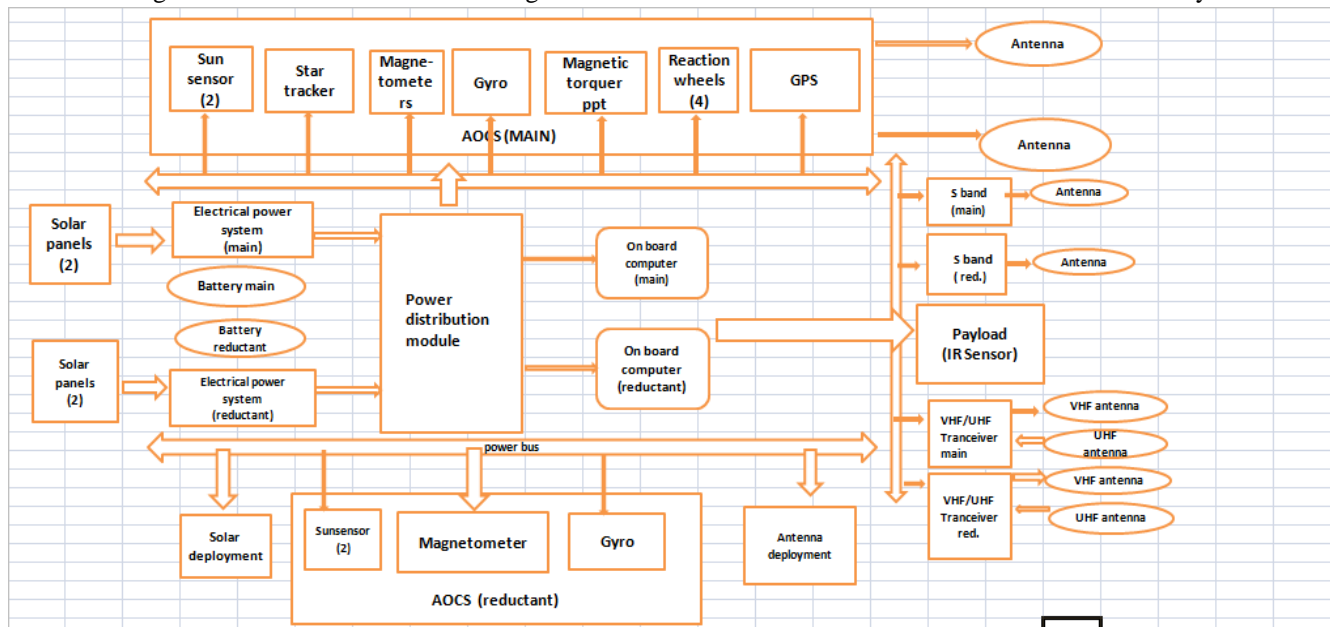


Fig.20 flow diagram of the overall arrangements of various components in astra nanosat

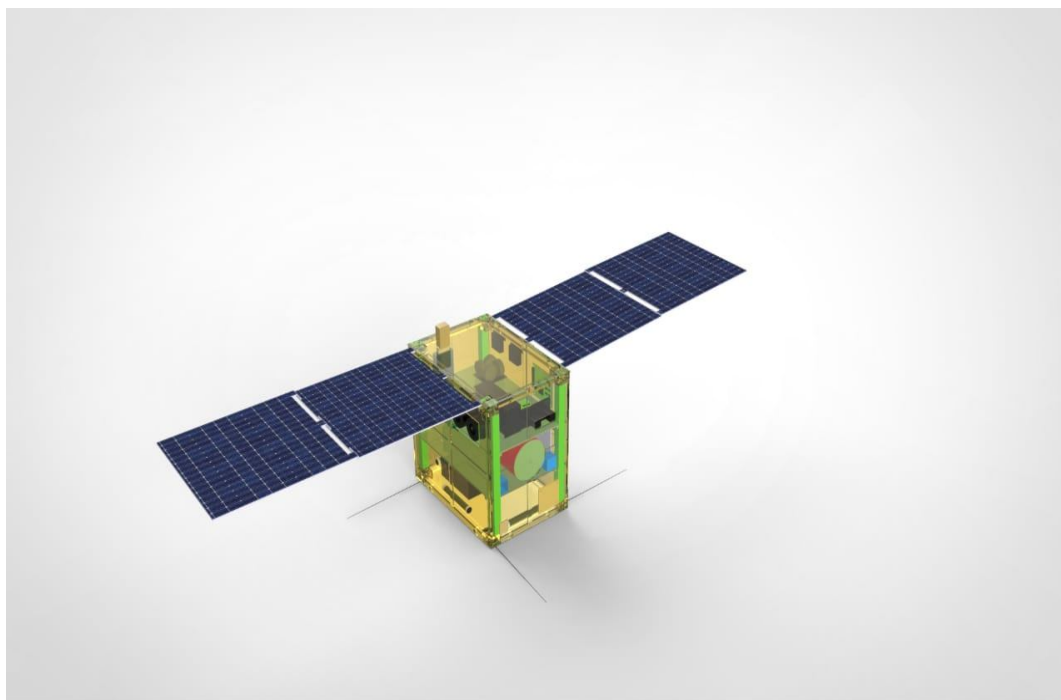


Fig.21 the rendered model of the nanosatellite done in key shot 7

**V. ANALYSIS**

The analysis of the designed nanosatellite in CATIA V5 has been done in the Nastran Patran software. (Riccard Benvenuto, 2016)[23] The analysis has done by selecting the various parameters for the satellite. The material used for the structure of the satellite is Aluminium 6061. The Overall weight of the satellite was estimated to be 13kg.

**TABLE II  
PROPERTIES OF ALUMINIUM 6061**

Properties	Values	Units
Density	2.70	g/cm <sup>3</sup>
Melting point	585	°C
Thermal expansion	23.5*10 <sup>-6</sup>	/K
Elastic modulus	70	GPa
Thermal conductivity	166	W/mK
Electrical resistivity	0.040*10 <sup>-6</sup>	Ωm
Tensile strength	260	MPa
Yield strength	240	Mpa
Brinell hardness	95	HB
Fatigue strength	97	MPa
Poisson's ratio	0.33	
Specific heat capacity	897	J/KgK
Resistivity	39.2	nΩm

**VI. RESULT OF ANALYSIS**

The analysis has been done as three stages by fixing the bottom panels and side panels simultaneously. The bottom panel of the satellite is going to be placed inside the launching pad of the launch vehicle, hence the analysis is also done by keeping the bottom panel fixed and loads are applied on the top. The analysis done for 11G that is 11G = 11\*13\*9.81

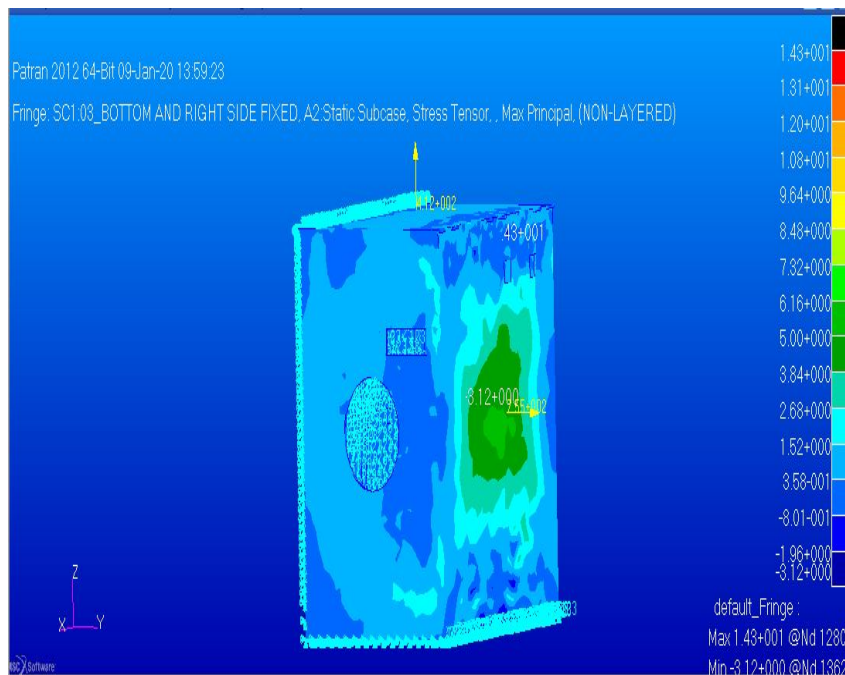


Fig.22 principal stress analysis by fixing bottom and right side wall

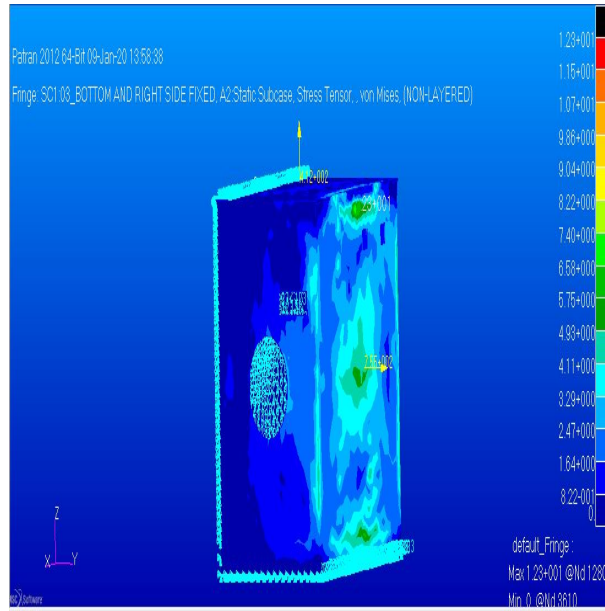


Fig.23 stress analysis of von mises by fixing bottom and left side walls

Figure 22 and 23 shows the results obtained from the stress analysis of the satellite by fixing the bottom walls and side walls. fig 22 shows the principal stress analysis result.

The maximum principal stress obtained is 1.43+001

The minimum principal stress obtained is -3.12

Fig23 shows the stress analysis result for von mises

The maximum stress tensor von mises is 1.23+001

The minimum stress tensor von mises is 0

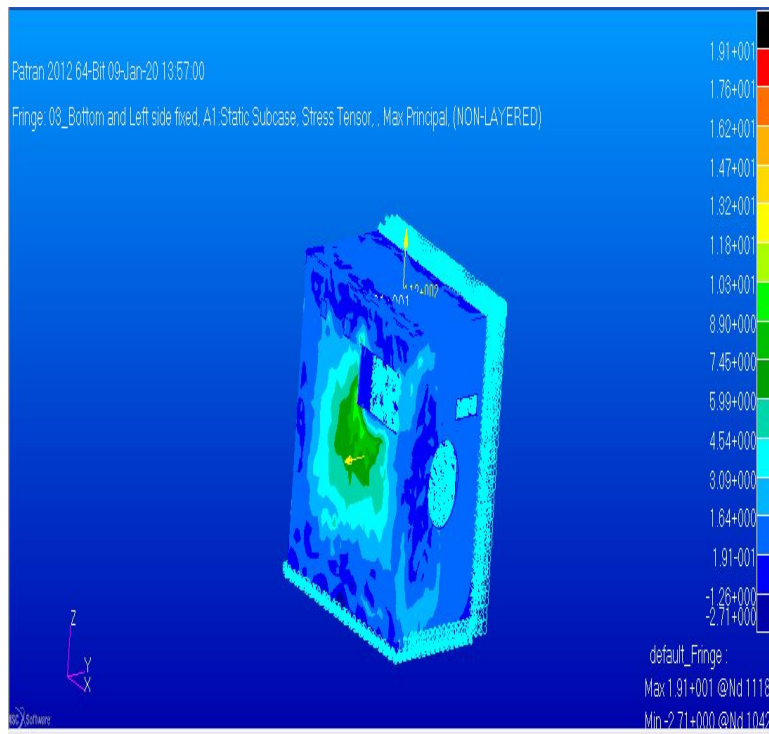


Fig.24 principal stress analysis by fixing bottom and left side walls

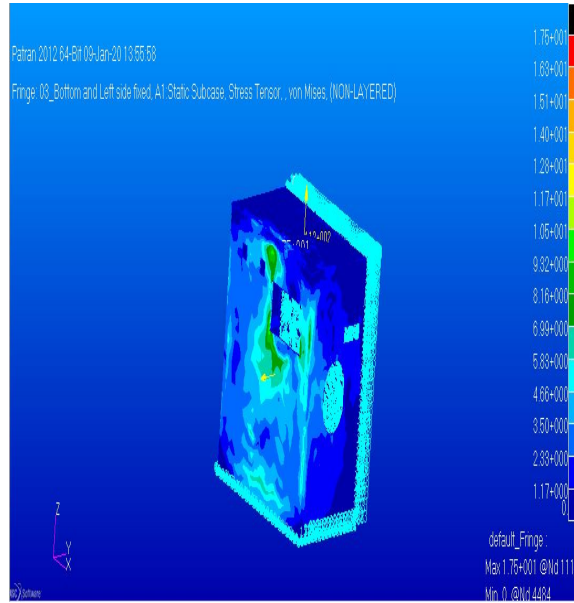


Fig.25 stress analysis for von mises by fixing bottom and left side walls

Figures 24 and 25 shows the stress analysis results when bottom and left side walls are fixed.

Figure 24 shows the stress analysis result obtained for principal stress

Maximum principal stress is 1.91+001

Minimum principal stress is -2.71

Figure 25 shows the stress analysis result obtained for von mises stress tensor

Maximum stress tensor von mises is 1.75+001

Minimum stress tensor von mises is 0

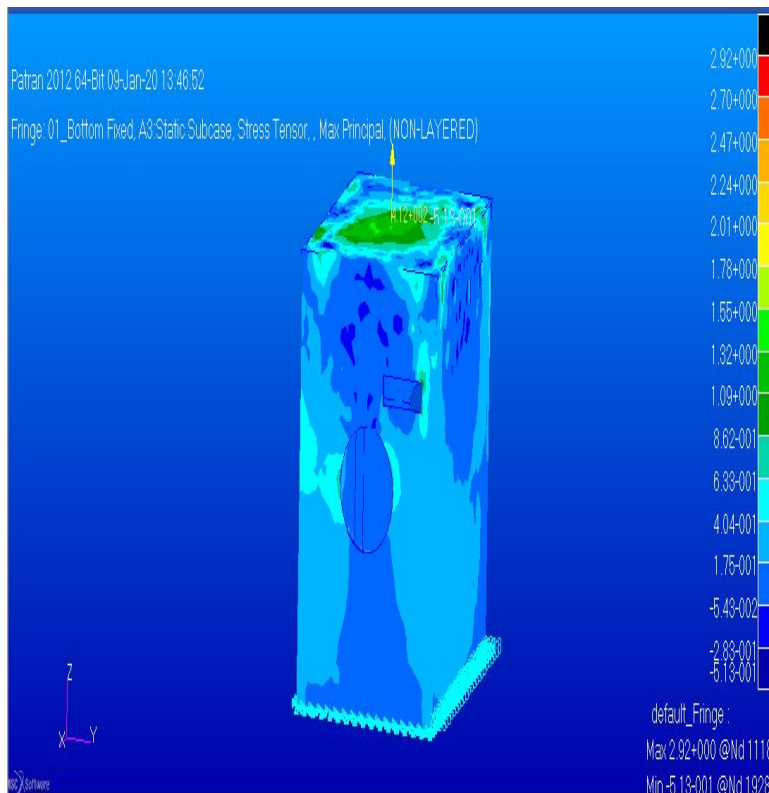


Fig.26 principal stress analysis by fixing bottom

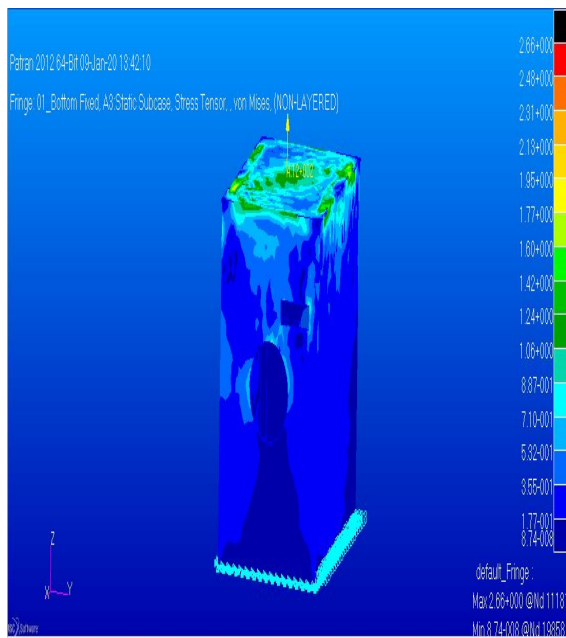


Fig.27 stress analysis for von mises by fixing bottom

Figure 26 and 27 shows the stress analysis results obtained when bottom is fixed and load conditions are applied on the top panel

Figure 26 shows the analysis results for principal stress

Maximum principal stress is 2.92

Minimum principal stress is -5.13-001

Figure 27 shows the analysis results for stress tensor von mises

Maximum stress tensor von mises is 2.66

Minimum stress tensor von mises is 8.74-008

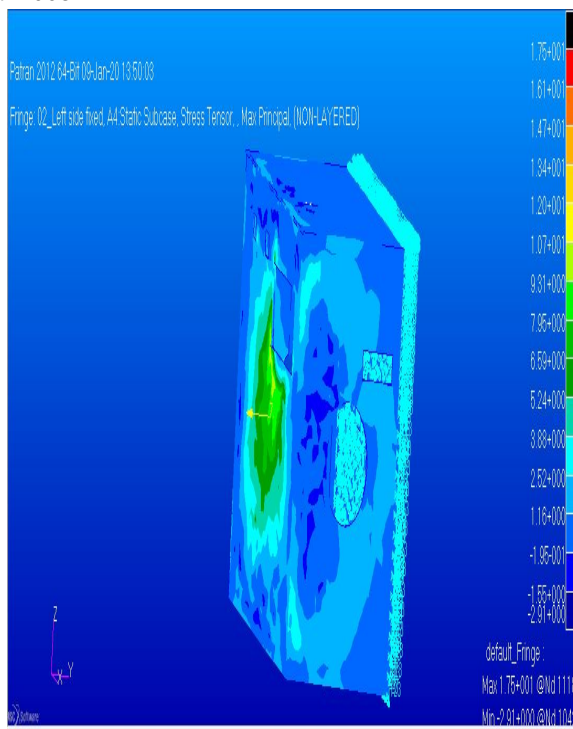


Fig.28 principal stress analysis by fixing left side wall

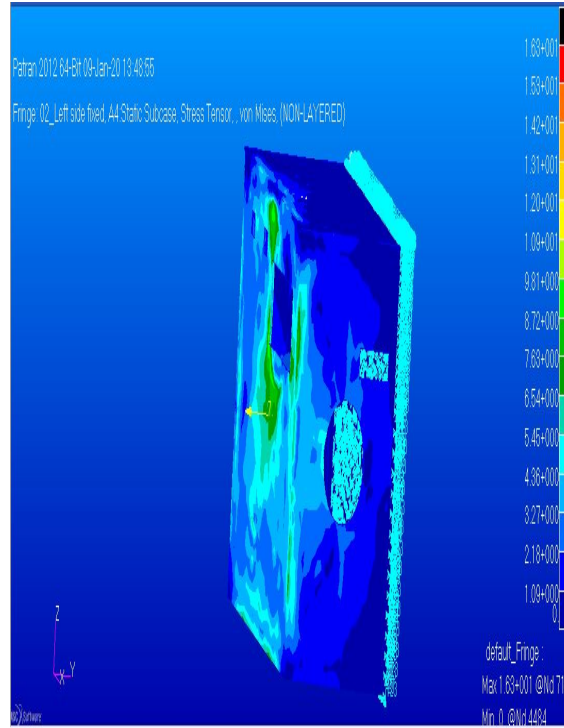


Fig.29 stress analysis for von mises by fixing left side wall

Figure 28 and 29 shows the results of stress analysis obtained when left wall is fixed and load conditions are applied on the other side.

Figure 28 shows the principal stress values

Maximum principal stress is  $1.75+001$

Minimum principal stress is  $-2.91$

Figure 29 shows the stress tensor von mises values

Maximum is  $1.63+001$

Minimum is 0

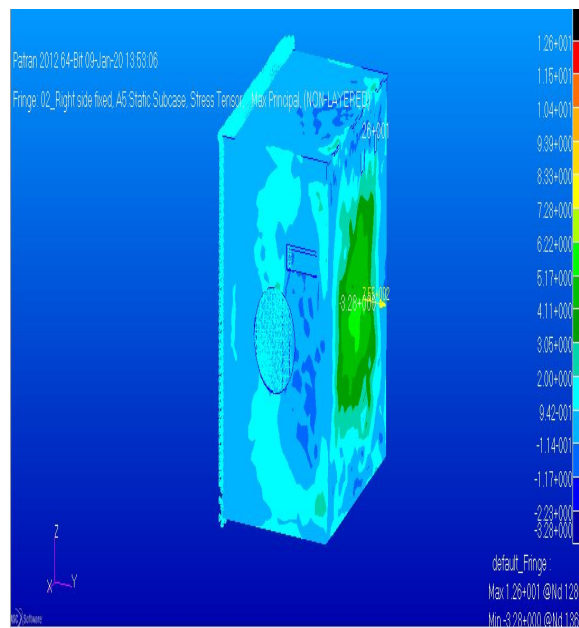


Fig.30 principal stress analysis by fixing right side wall

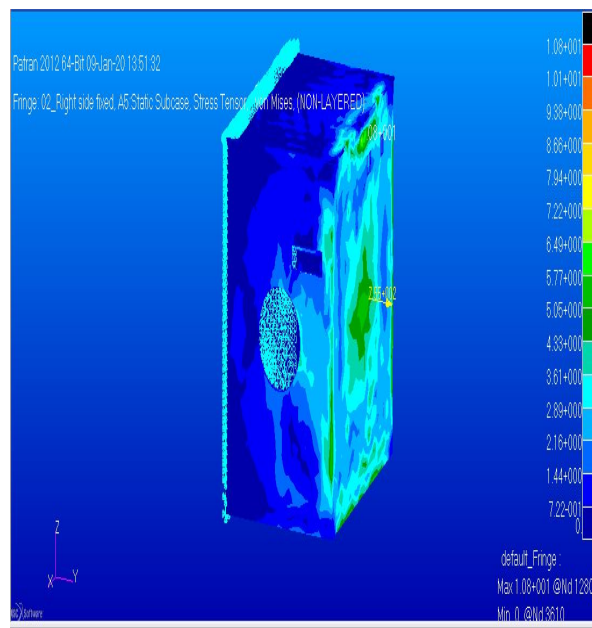


Fig.31 stress analysis for von mises by fixing right side walls

Figure 30 and 31 shows the results of stress analysis obtained when right side wall is fixed and load conditions are obtained

Figure 30 shows the result of stress analysis obtained for principal stress

Maximum principal stress is 1.26+001

Minimum principal stress is -3.28

Figure 31 shows the result for von mises

Maximum is 1.08+001

Minimum is 0

## VII. CONCLUSION

The design and analysis of the nanosatellite weighing 13Kilogram is completed using CATIA V5 software and Nastran Patran software. ASTRAA NANOSAT is able to detect the debris particle in Lower Earth Orbit. The selected orbit of ASTRAA NANOSAT is from 45 0Kilometer to 600Kilometer. The tether net is implemented with magnetic balls at the ends to capture the detected debris particles to an extent. The stress analysis of the satellite structure is done by fixing bottom and side panels at a time for 11 G condition. The maximum principal stress experienced by the satellite will be about 2.92 N/mm<sup>2</sup>. The Infrared sensor and Tether net implemented in the satellite is with an approximate weight relaxation of about 2Kilogram and 3 Kilograms respectively. Further research is required for the proper estimation of the weight of these two components. For the increment in the required power of the satellite, we can change the dimension of the cells in the solar panels. Since the stress experienced by the satellite when bottom fixed condition is low, the satellite is recommended to be placed in the launching pad of the launch vehicle by fixing the bottom panel.

## VIII. ACKNOWLEDGMENT

The authors would like to express their gratitude to the college, Noorul Islam Centre For Higher Education for sincerely supporting and helping to do this research paper.

## REFERENCES

- [1] Habimana Sylvestre, R. P. (2017). Space debris: reasons, types, impacts and management. Indian Journal of Radio and Space Physics , 20-26.
- [2] D Mahrholz, L. L. (2002). Detecting tracking and imaging space debris.
- [3] Christoph R Englert, J. T. (2014). Optical debris spotter. Acta Astronautical, 104 , 99-105.
- [4] Ansdell.M. (2010). Active space debris removal:needs,impication and recommandations for todays geopolitical environment. Journal of public and International affairs
- [5] K Wormnes, R. L.-M. (2013). ESA Technologies for space debris remediation. Sixth European Conference on space debris.
- [6] Shaobo Ni, C. Z. (2011). Attitude determination of nanosatellite based on gyroscope, sunsensor and magnetometer. Elsevier , 959-963.
- [7] Delabie, T. (2016). Star tracker algorithms and low cost attitude determination and control system for space mission. 1-185.



- [8] Halil Ersin Soken, S.-I. S. (2015). Magnetometer calibration for advanced small satellite mission. International Symposium on space technology and science, (pp. 1-7). Kobe.
- [9] Kikuko Miyata, J. C. (2009). Attitude control by Magnetic torquer. 1041-1060.
- [10] Shaobo Ni, C. Z. (2011). Attitude determination of nanosatellite based on gyroscope, sunsensor and magnetometer. Elsevier , 959-963.
- [11] Long, F. W. (2014). Design and testing of a Nanosatellite simulator reaction wheel attitude control system. 1-74.
- [12] Touhidul Alam, M. T. (2018). Design and Compatibility analysis of a solar panel integrated UHF antenna for Nanosatellite Space mission.
- [13] Erin Kahr, L. B. (2013). Design and operation of the GPS receiver Onboard the CanX-2 Nanosatellite. Navigation , 143-156.
- [14] Fabio Santon, P. T. (2002). Commercial Li-Ion Batteries for Nanosatellite applications- A flight experiment. Research Gate , 1-7.
- [15] Saurabh M Rajee, A. G. (2017). Development of onboard computer for a Nanosatellite. 68th International Astronautical Congress , 25-29.
- [16] M.T. Islam, M. S. (2015). Development of S band antenna for Nanosatellite. IEEE Asia-Pacific Conference on applied electromagnetics. Johor Bahru, Malaysia: IEEE.
- [17] Wilke, R. (2015). S band UHF and VHF communication system for cubesats including ground station software. Research gate , 1-20
- [18] A. Elmayh, A. P. (2017). Design and implementation of power distribution module of Lower earth orbit small satellite. IOSR journal of electrical and electronics engineering , 35-47.
- [19] Jie Liu, H. Z. (2012). Design of telemetry and telecommand sub systems of a microsatellite based on industrial level chips. International Journal of Circuit Systems and signal Processing , vol-6.
- [20] Eslava, S. A. (2014). Design of a micro pulsed plasma thruster for 3U cubesat. Research gate , 1-16.
- [21] Benjamin Thomas, I. S. (2016). Experiment on tethered capture and net closing mechanism of space debris. 67 th International Astronautical Congress , IAC-16-A6.6.7.
- [22] Jonathan Becedas, A. C. (2018). Additive manufacturing applied to the design of small satellite structure for space debris deduction.
- [23] Riccard Benvenuto, S. S. (2016). Dynamics Analysis and GNC design of flexible systems for space debris active removal. IAA-AAS-DyCoss2-14-09-02 , 17-30.
- [24] al, C. P. (2019). Review of active space debris removal techniques. Space Policy , 194-206.
- [25] al, G. F. (2013). Satellite configuration design. Finite Element for Satellite Structure , 1-4471.
- [26] Alesandro Rossi, C. C. (2015). ReDSHIFT: A global approach to space debris mitigation.
- [27] Brijesh Patel, K. P. (2017). A critical review on space disposal techniques for space debris. JGEESI , DOI:10.9734.
- [28] Bryce Barcelo, E. S. (2012). Space Tethers: Applications and Implementations. Worcester Polytechnic Institute in Partial Fulfillment of Requirements for the degree of Bachelor of Science, PKA-SB07 .
- [29] Burgess, M. N. (2014). Active space debris removal inevitability. The Royal Canadian Airforce Journal , 7-17.
- [30] Chaddha, S. (2011). Space Debris Mitigation- Revised . SSRN , 22.
- [31] Claude R Phipps, K. L. (2014). Removing Orbital Debris with Lasers. United states department of energy's National Nuclear Security Allocation , DE-AC04-94AL85000.
- [32] Florio Della Vedova, P. M. (2018). Interfacing sail modules for use with space tugs.
- [33] hall, L. (2014). The history of space debris. Space traffic management conference .
- [34] Hobbs, S. (2010). Debris removal from lower earth orbit DR LEO. College of Aeronautics Report , 1001.
- [35] J C Liou, N. L. (2007). A Sensitive study of the effectiveness of active debris removal in LEO. In 58 th International Astronautical Congress , 236-243.
- [36] Katharine M Brumbaugh, H. C. (n.d.). In situ Sub-millimeter space debris detection using cubesats.
- [37] M Andrenucci, P. A. (2011). Active removal of space debris expanding form application for active debris. University of PISA,ACT .
- [38] M R Lavagna, R. A. (2012). Debris removal mechanism using tethered nets. Research gate .
- [39] M S Rhee, C. M. (2014). Highlights of Nanosatellite propulsion development programme at NASA-Goddard Space Flight center. USU conference on small satellites , 1-1.
- [40] Mahdi, M. C. (2015). Orbit Design and Simulation for KUFASAT Nanosatellite. Artificial satellites , 4-2915.
- [41] Marc Thillot, Z. B. (2007). Microsatellite for space debris observation by optical sensors. International Conference on Space Optics .
- [42] Pedro Velez, T. A. (2017). Space debris removal using a tether: A Model. International Federation on Automatic Control , 7247-7252.
- [43] (2013). preliminary design review document for NIUSAT telemetry telecommand and communication system(TTC). NICHE.
- [44] R Lucken, N. H. (2017). Systematic Space debris collection using cubesat constellation. 7th European Conference for Aeronautics and Aerospace Sciences(EUCASS) .
- [45] Sam Harrison, P. S. (2012). Nanosatellite fabrication and analysis.
- [46] Shang, S. B.-R. (2018). Space debris removal mechanism using cubesat using gunshot method.
- [47] Tam, W. (2015). The space debris Environmental and satellite manufacturing. Walden Dissertations and Doctoral studies and Scholar works , 1-183.



10.22214/IJRASET



45.98



IMPACT FACTOR:  
7.129



IMPACT FACTOR:  
7.429



# INTERNATIONAL JOURNAL FOR RESEARCH

IN APPLIED SCIENCE & ENGINEERING TECHNOLOGY

Call : 08813907089  (24\*7 Support on Whatsapp)